Science and Technology Indonesia
e-ISSN:2580-4391 *p*-ISSN:2580-4405
Vol. 8, No. 1, January 2023

Research Paper

Fe_3O_4-SiO_2-Alginate Photocatalyst for Textile Dyes Waste Degradation

Sri Wardhani[1*], Herdian Akbar Mardiansyah[1], Danar Purwonugroho[1]

[1]*Faculty of Mathematics and Natural Sciences, Brawijaya University, Malang, 65145, Indonesia*
***Corresponding author**: wardhani@ub.ac.id*

Abstract
Fe_3O_4 is a photocatalyst that is used to degrade textile dye waste which can be collected and reused. Fe_3O_4 was prepared by coprecipitation method, then impregnated with SiO_2 and sodium alginate. The purposes of this study were to investigate the degradation of textile dye waste using a Fe_3O_4-SiO_2-alginate photocatalyst, to examine the light and dark test of photocatalyst under the influence of concentration and irradiation time. The type of light used was a 14.5-watt Philips LED lamp with a wavelength of 400-640 nm. Photocatalyst characterizations were conducted using FTIR, UV-Vis DRS, and XRD. The light and dark test of photocatalyst was carried out by photodegradation of textile dye waste with 0.5 g of photocatalyst with concentrations of 5%, 10%, and 15% and irradiation times were varied for 60, 90, 120 min. The degradation results were measured by calculating the COD value. The results of characterization by FTIR showed that the photocatalyst Fe_3O_4-SiO_2-Alginate had absorption at wavelengths of 637.56 cm^{-1} and 3365.86 cm^{-1} which indicated the Fe-O-Si functional group and O-H stretching vibration. Results of UV-Vis DRS were analyzed using Origin Pro 2022 and revealed that the band energy gap for Fe_3O_4 and Fe_3O_4-SiO_2 were 2.20 eV and 1.77 eV, respectively. The XRD results analysis with Match!3 software showed that for Fe_3O_4 had magnetite phases, while SiO_2 had amorphous cristobalite phases. The 15% (w/v) Fe3O4 concentration in the form of powder and granules degraded batik liquid waste by 79.6% and 84.48%, respectively.

Keywords
Textile Waste, Photocatalyst, Fe_3O_4, SiO_2, Chemical Oxygen Demand (COD)

Received: 18 Oktober 2022, Accepted: 5 January 2023
https://doi.org/10.26554/sti.2023.8.1.108-115

1. INTRODUCTION

Fe_3O_4 iron oxide photocatalyst prepared by coprecipitation using $FeCl_3.6H_2O$ and $FeCl_2.4H_2O$ precursors at 25°C and pH = 10 has an energy gap nanoparticles of 2.22 eV (Saragi et al., 2018). Fe_3O_4 nanoparticles were prepared by coprecipitation method. $FeCl_3$ and $FeSO_4{\cdot}7H_2O$ (with a molar ratio of 2:1) were dissolved in 100 cm^3 of water and a modifier was added. Optical band gap energy values to be synthesized by co-precipitation of magnetite nanoparticles was 2.51-3.01 eV (1.band gap). The synthesized Fe_3O_4 thin film synthesis has a band gap, energy band gaps (EgOpt) determined fromUV visible (UV–vis) measurements indicated the increase of indirect ($2.17 \leq Eg1Op \leq 2.25$ eV) and direct ($2.78 \leq Eg2Op \leq 2.95$ eV) band gap of Fe_3O_4 (Kouotou et al., 2018). Several methods to synthesize Fe_3O_4 are coprecipitation method Ardiyanti et al. (2019), thermal decomposition, microemulsion and hydrothermal method (Asab et al., 2020; Hedayati et al., 2017). The coprecipitation method is the easiest method to apply and high yields are obtained which depend on the precipitation and reduction of iron III hydroxide and iron II hydroxide. The deposition process is influenced by acidity conditions and the ratio of moles of Fe^{3+}/Fe^{2+} used (Villegas et al., 2020). Iron oxide photocatalyst has been used to degrade some synthetic dyes, but the ability of this photocatalyst is very dependent on neutral pH because it is easy to photo reduce which can interfere with the photodegradation process. Fe_3O_4 must be modified by adding a barrier layer to reduce photo dissolution, hydrolysis, and oxidation. An example of a barrier material that can be used is SiO_2 which has stable physical properties, a large surface area, and can maintain the effectiveness of Fe_3O_4 (Madima et al., 2022).

The activity of photocatalysts can be increased through the addition of SiO_2 which is beneficial for increasing the surface area of the available catalyst, allowing for increased adsorption of pollutant molecules (Mohammadi and Sabourmoghaddam, 2019). Silica as a supporting material in the field of photocatalysis is proven to increase its performance and potential as an antibacterial agent (Luthfiah et al., 2021). The Fe_3O_4 photocatalyst is formed into granules with the addition of alginate to facilitate the photodegradation process. Alginate is widely used as thickening agent, gelling agent, and emulsifier because

the material is non-toxic, simple to use, does not require special equipment, is non-toxic, economical, and can also be a protective material supporting SiO_2 (Nisaa et al., 2018). An optimal amount of catalyst in wastewater treatment is required to prevent excess catalyst and ensure efficient absorption of total photons. Paraquat degradation has been investigated by loading the catalyst in solution at 0.1–2 g/L (Gunlazuardi et al., 2021). The increase in catalyst mass up to 300 mg/L causes the decolorization process to increase as well. This is related to the increase in active sites on the surface of the catalyst so that it can accelerate the decolorization process (Al-Anbari et al., 2016).

Natural materials that can be used to obtain silica is rice husk, with a SiO_2 content of up to 80%. Some inorganic compounds contained in rice husks are potassium, sodium, calcium in small amounts and also silica in higher amounts (Fatimah et al., 2021). Silica extraction methods, namely thermal and non-thermal methods. For non-thermal methods, one of them is washing with acid in order to remove organic compounds and other metal impurities from rice husks. Silica extracted from rice husk by leaching with HCl showed a purity of 95.48% (Kamari and Ghorbani, 2021).

Based on previous research, Fe_3O_4 nanoparticles have a large surface volume ratio of about 20 nm ((Ta et al., 2016). The large surface volume ratio causes high surface energy which leads to particle aggregation. In addition, Fe_3O_4 has a high chemical activity on its surface, making it susceptible to air oxidation which then causes its magnetic properties and dispersibility to decrease. Therefore, it is necessary to modify Fe_3O_4 with various materials such as polymers, silica, carbon, oxide absorbers, metal oxides, or luminescent materials. Based on the previously mentioned, inorganic materials such as silica (SiO_2) are considered to meet the requirements to overcome these problems. The increase in SiO_2 content causes the energy gap in the sample to be smaller. The band gap energy of the sample is inversely proportional to the particle size. The band gap energy value describes the amount of energy required to excite electrons from the valence band to the conduction band. High band gap values require more energy for electron excitation, so high light frequencies and low wavelengths will be absorbed (Nikmah et al., 2019).

Alginate is often used as a thickener, gelling agent, stabilizer and emulsifier which has an important role in the food industry, textile printing industry and batik printing. Alginate can undergo the substitution of Na^+ ions with polyvalent cations Ca^{2+} which causes the formation of granules with a stable structure formed through cross-linking interactions. This interaction is used to bind the molecules of the photocatalyst to form a granule to make it more efficient (Bayat et al., 2018). The use of alginate as a stabilizer allows the production of ultrafine nanoparticles on the order of -2-5 nm. The use of alginates for catalytic applications has shown promising results in the reduction of MB dyes (Benali et al., 2021).

Previous studies have focused on photocatalysts in powder form even though they have been coated with SiO_2. Therefore, the research is interested in examining photocatalysts in the form of granules which are expected to have the same photocatalytic activity compared to powder forms for photodegradation of liquid waste.

2. EXPERIMENTAL SECTION

2.1 Materials

The materials used in this study were rice husk, distilled water, 37% technical HCl, $FeSO_4.7H_2O$ (Merck), $FeCl_3.6H_2O$ (Merck), NH_3 (Merck), Sodium Alginate, $HgSO_4$ (Merck), 98% H_2SO_4 (Merck) , $K_2Cr_2O_7$ (Merck) and $(NH_4)_2Fe(SO_4)_2$ $6H_2O$ (Merck), Textile Dyes Waste was collected from Rumah Batik Pandan Arum, Malang. The tools used in this research are Philips LED lamps 14.5 watts and a reflux device. Meanwhile, for the analysis of the results of synthesis and photodegradation, the instruments used include the Shimadzu Infrared Spectrophotometry (FTIR) instrument with type 8400S, Analytical UV-Vis Spectrophotometer Jena Specord 200 plus, XRD PANalytical X'Pert Pro.

2.2 SiO_2 Isolation from Rice Husk

Rice husks is washed, air-dried and then dried in the oven. Furthermore, the rice husks were ashed at a temperature of 700°C for 4 hours. The cooled rice husk ash was then dissolved into 3 M HCl solution with a ratio of 1:3 (w/v) at 75°C for 4 hours. After being separated from the filtrate, the filtered residue was washed with distilled water until the pH of SiO_2 was the same as that of distilled water and then dried.

2.3 Synthesis of Fe_3O_4

The synthesis process was carried out by dissolving $FeSO_4.7H_2O$ and $FeCl_3.6H_2O$ with a mole ratio of 1:2 (4.17 g; 8.109 g) into 30 mL distilled water. Furthermore, 60 mL of 10% NH_4OH solution was added to the solution by dripping slowly and stirring over a magnetic stirrer for 90 minutes at a temperature of 60°C with a stirring speed of 450 rpm. The Fe_3O_4 solution then washed with distilled water. After that, the Fe_3O_4 deposition process was carried out. Fe_3O_4 solution placed on an external magnet (permanent magnet), then washed with distilled water for ±7 repetitions. The precipitate that has been washed and then dried was heated in an oven at 100 $\frac{238}{92}$C for 2 hours, then grounded with a spatula until became powder.

2.4 Fe_3O_4-SiO_2 Composite Preparation.

0.05 g of Fe_3O_4 was added with 30 mL of 96% ethanol in a 100 mL beaker, then stirred using a magnetic stirrer for 1 hour. Then 0.95 g of SiO_2 was added to the mixture and stirred for 3 hours at 30°C, then the Fe_3O_4:SiO_2 ratio was varied by 10% and 15% (w/w) for a total of 1 g, respectively. The Fe_3O_4-SiO_2 precipitate was dried and calcined at 500°C for 4 h.

2.5 Synthesis of Fe_3O_4-SiO_2-Alginate Photocatalyst

The Fe_3O_4-SiO_2 photocatalyst was impregnated with sodium alginate gel to make the adsorbent in the form of granules in calcium chloride solution. A-2 g of sodium alginate was

© 2023 The Authors.

dissolved in 13 mL of distilled water, stirred using a magnetic stirrer while heated at 40°C to form a gel phase. A-3 g of Fe_3O_4-SiO_2 was crushed using a mortar and then mixed into the alginate gel. The suspension was then injected into a 10% (w/v) calcium chloride solution with a syringe. The granules of the Fe_3O_4-SiO_2-Alginate complex formed were then separated and dried at 120°C to dryness.

2.6 Photocatalyst Test with Light and Without Light

Five 50 mL beakers were filled with 25 mL of textile dye waste with different treatments, namely the first glass containing a textile dye waste solution; the second glass added 50 mg Fe_3O_4; the third glass added 50 mg SiO_2; the fourth glass was added 50 mg Fe_3O_4-SiO_2 and the fifth glass was added 50 mg Fe_3O_4-SiO_2-Alginate. Then the photodegradation process was carried out without sunlight for 60 minutes. Furthermore, with the same preparation procedure, a 14.5watt Philips LED lamp was irradiated. Furthermore, the solution was analyzed for its COD value.

2.7 Effect of Fe_3O_4-SiO_2-Alginate Concentration on Batik Waste Degradation

Three beakers were filled with 25 mL of textile dye waste and added 50 mg of photocatalyst with varying concentrations of Fe_3O_4-SiO_2 by 5%; 10%; and 15% (w/w) then irradiated with a 14.5 watt Philips LED lamp for 60 minutes and the solution was analyzed for its COD value.

2.8 Chemical Oxygen Demand Test

Textile dyes waste was first measured for its COD by taking 10 mL and putting it into a round bottom flask. Then added 10 mL of $K_2Cr_2O_7$ 0.25 N, 10 mL of 9 M H_2SO_4, 25mL of distilled water, and a small amount of $HgSO_4$ powder into a round bottom flask. The round bottom flask containing the solution mixture was arranged in a reflux apparatus with a condenser using a stream of cold water. Then the solution was refluxed for two hours at 100 $\frac{238}{92}$C. Wait for the solution cool and then add 2 drops of Ferroin indicator. The solution is then titrated with 0.25 N FAS and the volume of the titration is recorded. After doing the same treatment for the waste that has been degraded with photocatalyst.

The activity test was carried out to calculate the COD value of textile waste before irradiation, the results of the activity test of textile wastewater treated with variations in the concentration of Fe_3O_4-SiO_2 in the Fe_3O_4-SiO_2-alginate photocatalyst and the duration of irradiation from the degradation of textile dyes waste. COD calculation is carried out with the following formula (1)

$$\text{COD} = \frac{(\text{b-a}) \times \text{BeO}_2 \times \text{P}}{\text{V}} \quad (1)$$

Where Exp: b (titration sample volume), a (titration blank volume), P (dilution factor), Be O_2 (Equivalent Mass O_2), N (Normality FAS), V (sample volume). Then, waste degradation percentage is carried out with the following formula (2)

$$\%\ \text{Degradation} = \frac{(\text{C before- C after})}{(\text{C before})} \times 100\% \quad (2)$$

Where Exp: C before (COD value before COD test), C after (COD value after COD test) (Tak et al., 2015).

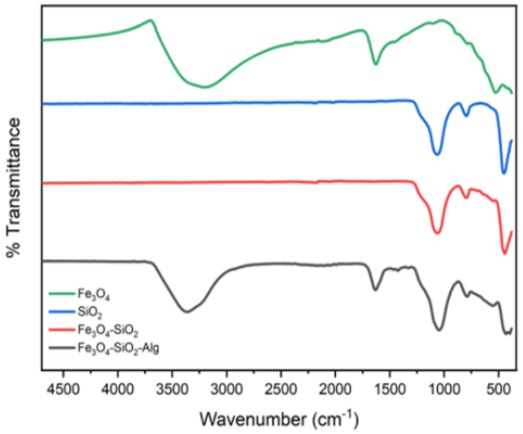

Figure 1. FTIR Spectra of Photocatalyst

2.9 Characterizations

UV Vis Diffuse Reflectance (DRS) generate %R which is converted into R (reflectant value). kubelka munk factor with the following equation (3)

$$\text{F(R)} = \frac{\text{K}}{\text{S}} = \frac{1 - \text{R}^2}{2\text{R}} \quad (3)$$

Where Exp: F(R) (Kubelka-Munk Factor), K (absorption coefficient), S (scattering coefficient), R (Reflectance value). XRD for phase analysis of photocatalyst materials, analyzed using Match! 3 (Nikmah et al., 2019).

3. RESULT AND DISCUSSION

3.1 Characterization Using FTIR Spectroscopy

Based on Figure 1 and Table 1, SiO_2 spectra showed absorption at a wave number of 452.11 cm^{-1} indicating the Si-O functional group, then 795.83 cm^{-1} and 1062.53 cm^{-1} indicating the presence of Si-O bonds. Fe_3O_4-SiO_2-Alginate showed absorption at a wave number of 556.22 cm^{-1} which indicated the presence of a Fe-O functional group, then 637.56 cm^{-1} indicated the presence of Fe-O-Si bonds, and 430.72 cm^{-1}, 790.12 cm^{-1}, 1046.84 cm^{-1} respectively indicate the presence of Si-O bonds.

3.2 Characterization Using UV-Vis DRS

Characterization using UV-Vis DRS aims to determine the band gap energy of Fe_3O_4 and Fe_3O_4-SiO_2. The band gap energy of Fe_3O_4 is calculated to determine how much bandgap energy is produced from the synthesized Fe_3O_4, while the

© 2023 The Authors.

Table 1. IR Interpretation

Fe_3O_4	SiO_2	Fe_3O_4- SiO_2 cm^{-1}	Fe_3O_4- SiO_2-Alginate	Interpretation	References
3208.98	-	-	3365.86	O-H Stretch	(Nikmah et al., 2019)
1628.73	-	-	1631.59	O-H Bend	(Nikmah et al., 2019)
-	1062.53	1063.54	1046.84	Si-O Stretch	(Nikmah et al., 2019; Chang et al., 2022)
-	795.83	797.25	790.12	Si-O Bend	(Chang et al., 2022; Gong and Tang, 2020)
-	-	634.66	637.56	Fe-O-Si	(Gong and Tang, 2020)
526.27	-	546.24	556.22	Fe-O Vibration	(Gong and Tang, 2020)
-	452.11	443.55	430.72	Si-O Asyym Bend	(Chang et al., 2022)

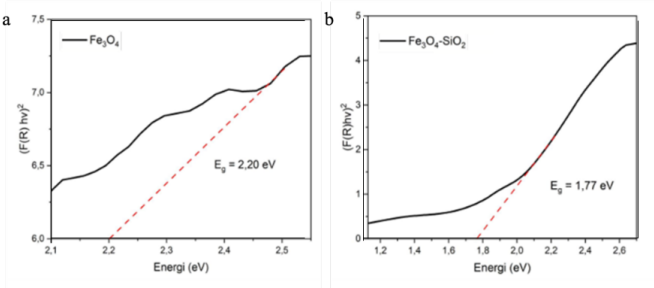

Figure 2. Band Gap Energy of: (a) Fe_3O_4; and (b) Fe_3O_4-SiO_2

band gap energy of Fe_3O_4-SiO_2 is calculated to determine the effect of the SiO_2 carrier. Based on the calculation of the characterization results, the bandgap energy value of the synthesized Fe_3O_4 is 2.2 eV where the results are in accordance with the research conducted by Saragi et al. (2018) which obtained the bandgap energy value of the synthesized Fe_3O_4 of 2.22 eV (Figure 2). Then Fe_3O_4 embedded in SiO_2 has a band gap energy of 1.77 eV. Based on Nikmah et al. (2019), the bandgap energy of Fe_3O_4 which has been treated with SiO_2 has decreased the bandgap energy according to the concentration variation of its composition.

The decrease in the band gap makes it easier for electrons to be excited from the valence band to the conduction band so that if the band gap energy is getting smaller, the energy required to make electrons excited to produce hydroxyl radicals is also smaller (Thiyagarajan et al., 2018). Hydroxyl radicals are strong oxidizing agents that function to reduce organic waste into water and carbon dioxide.

3.3 Characterization Using XRD

Qualitative characterization using XRD was carried out to determine the crystallinity based on the peaks and intensity on the diffractogram formed from the photocatalyst. In addition, XRD used to determine the dominant phase in the modification of Fe_3O_4 semiconductor material with SiO_2 embedded and then the results of the analysis are compared to PDF in the Match! 3 to identify the crystalline phases from sample (Keshavarz et al., 2019). The characterization results in Table 2 show the presence of Fe_3O_4 No. 96-722-8111 in the Fe_3O_4 sample shown at the visible peak. After being impregnated with SiO_2, the Fe_3O_4 peak did not change, indicating that the addition of a carrier did not damage the crystal structure.

Based on analysis with Match! software 3 obtained a Fe_3O_4 diffractogram which can be seen in Figure 4 where the characterization results show that there are magnetite and maghemite phases. The magnetite phase can be shown at 2θ peak of 30.21° ; 35.57° ; 37.15° ; 43.27° ; 53.71° ; 57.13° ; and 62.67° with Miller's index (202), (311), (222), (400), (422), (511), and (404). This phase can be shown based on the results of the comparison of the sample to PDF Magnetite No. 96-722-8111. The maghemite phase is shown based on the results of the comparison of the sample to PDF Maghemite No. 96-900-6317 with 2θ equal to 30.402° ; 35.6° ; and 43.531°.

The SiO_2 characterization showed the presence of cristobalite phase but it was amorphous (Figure 3) which was shown at the peak of 2θ of 17.53°; 21.81°; 24.93° with Miller index (110), (111), and (200). The cristobalite phase can be shown after doing a comparison between the SiO_2 sample and the PDF of Cristobalite No. 96-101-0922. The SiO_2 obtained is in accordance with the results of Sapei et al. (2015) where the peak of amorphous SiO_2 is at 2θ of 22°. The XRD pattern of silica was synthesized from rice husk waste with various concentrations of sodium hydroxide and acidification method with maximum intensity at 2θ = 22°. Silica obtained by alkaline extraction and acidification is completely amorphous (Dhaneswara et al., 2020).

Figure 5 shows theFe_3O_4/SiO_2 diffractogram, the presence of Fe_3O_4 indicated a peak at 2θ at 30.21°, 37.13°; 43.37° ; 57.13° ; and 62.97°. Figure 6 shows the diffractogram of SiO_2, Fe_3O_4, and Fe_3O_4/SiO_2. Based on Figure 6 and Table 2, it shows that 2θ of Fe_3O_4/SiO_2 still shows the peak of each compound. Result of characterization of Fe_3O_4 with SiO_2 showed the presence of Fe_3O_4 at the peak of 2θ at 30.21°, 37.13°; 43.37° ; 57.13° ; and 62.97° which is relatively the same as Fe_3O_4, and there is a peak of SiO_2 at 2θ of 21.62°. Then, based on the results of the comparison between Fe_3O_4 and SiO_2 samples, it showed the success of adding SiO_2 carriers through impregnation with the emergence of carrier peaks on the diffractogram (Song et al., 2013).

Based on the Debye-Scherrer equation, the crystal sizes of

© 2023 The Authors.

Table 2. Comparison of 2θ Between Fe_3O_4, SiO_2 and Fe_3O_4-SiO_2

Fe_3O_4	SiO_2	Fe_3O_4- SiO_2	PDF Fe_3O_4 Magnetite No. 96-722-8111	PDF SiO_2 Christobalite No. 96-101-0922	PDF Fe_2O_3 Maghemite No. 96-900-6317
-	17.53	18.13	-	17.53	-
-	21.81	21.62	-	21.51	-
-	24.93	23.87	-	24.83	-
-	27.67	27.71	-	27.83	-
30.12	-	30.21	30.33	-	30.402
35.57	-	35.67	35.55	-	35.6
37.15	-	37.13	36.97	-	-
43.27	-	43.37	43.27	-	43.351
53.71	-	53.69	53.69	-	-
57.13	-	57.13	57.19	-	-
62.67	-	62.97	62.97	-	-

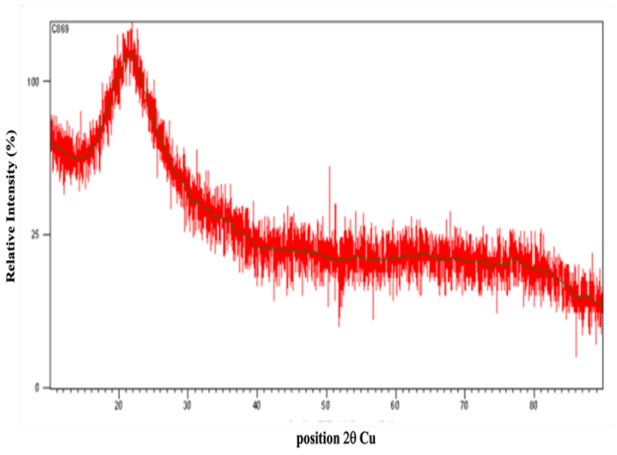

Figure 3. Diffractogram of SiO_2

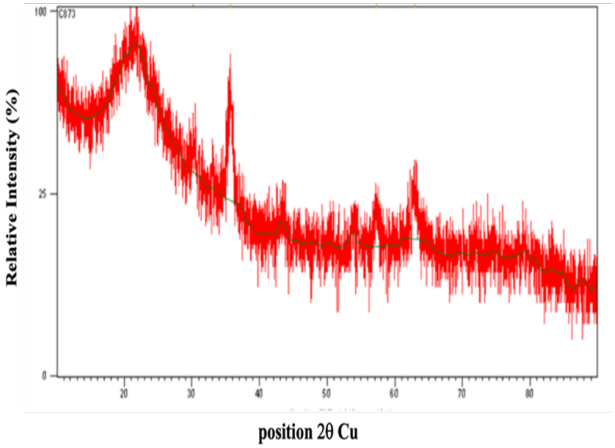

Figure 5. Diffractogram of Fe_3O_4- SiO_2

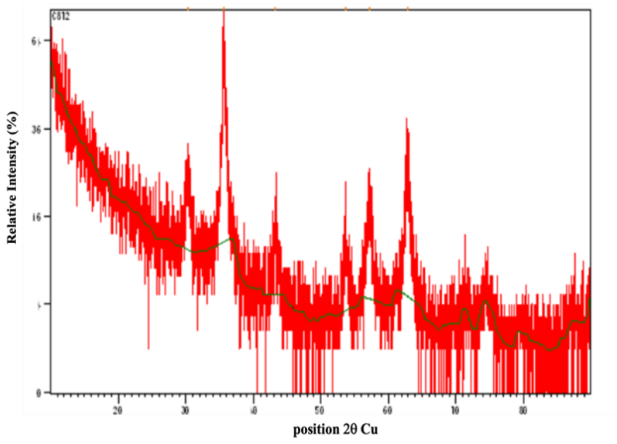

Figure 4. Diffractogram of Fe_3O_4

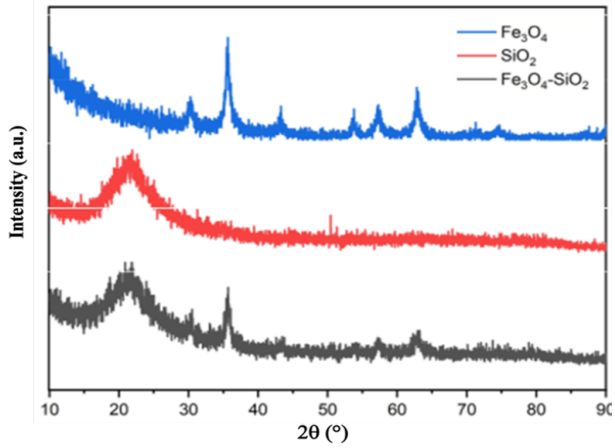

Figure 6. Diffractogram Fe_3O_4, SiO_2, and Fe_3O_4-SiO_2

© 2023 The Authors.

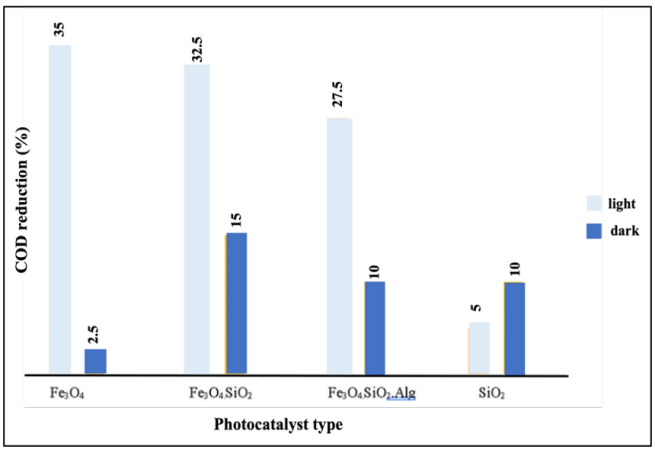

Figure 7. The Correlation of the Types of Photocatalyst to the Decrease in COD value (%) with Irradiation for 60 Minutes (Light) and Without Irradiation (Dark)

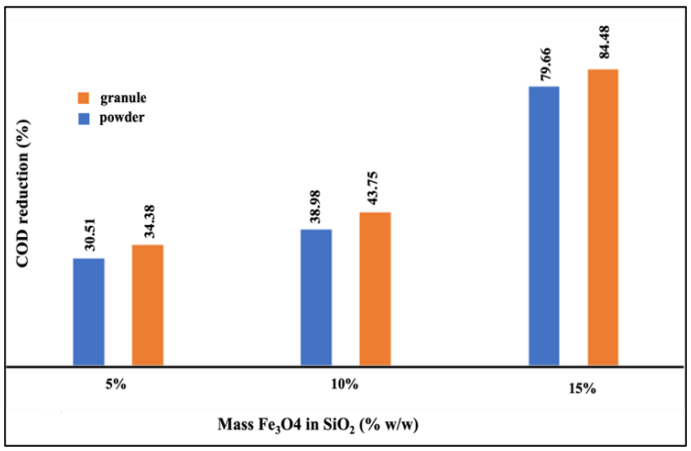

Figure 8. Relationship of Fe_3O_4 Concentration (w/w) to the Decrease in COD Value (%) of Textile Dye Waste with 60 Minutes of Irradiation

Fe_3O_4, SiO_2, and Fe_3O_4-SiO_2 were 97.35, respectively; 3.56; and 5.03 nm while the modified Debye-Scherrer was 69.19; 3.56; and 2.47 nm.

3.4 Photocatalyst Activity Test with Light and Without Light

Tests with and without light were carried out to determine the ability of photocatalysts to degrade textile dye waste in reducing the COD value of textile dye waste. The volume of textile dye waste used was 25 mL, 0.5 g of photocatalyst with a treatment duration of 60 minutes, namely with light and without light. At the time of initial measurement, the COD value of the waste before photodegradation was 800 mg/L. Fe_3O_4 in light can reduce the COD value by 280 mg/L and in the dark by 20 mg/L, this proves that the performance of Fe_3O_4 is very good under light. Then for SiO_2 when light and dark are 40 mg/L and 80 mg/L, respectively, which proves that SiO_2 acts as an adsorbent.

In the test results can be seen in Figure 7, the decrease in COD value with photocatalyst is influenced by light where Fe_3O_4 gives the highest COD value decrease of 35%, this indicates a photocatalytic reaction originating from Fe_3O_4 photocatalyst produces holes (h+ vb) and electrons (e)- (b). Hole reacts with H_2O to form OH or hydroxyl radicals which can degrade dyes (Yuliasari et al., 2021). Meanwhile, the decrease in COD value with SiO_2 is very small because SiO_2 is not a photocatalyst. Fe_3O_4 resulted in the greatest decrease in COD value because the photocatalyst material worked very well with the help of irradiation. After Fe_3O_4 was embedded in SiO_2, the decrease in COD value was slightly lower than that of Fe_3O_4, so it can be concluded that with the addition of SiO_2, the cost of using Fe_3O_4 photocatalyst semiconductor material can be reduced. In the treatment of textile dye waste with the addition of all photocatalysts used without irradiation gave a small decrease in COD value, namely 15% for Fe_3O_4-SiO_2. This provides information that no photocatalytic reaction occurs, but indicates that SiO_2 acts as an adsorbent. Treatment without irradiation makes Fe_3O_4 ineffective in forming hydroxyl (OH), because there is no photon energy from visible light that hits Fe_3O_4. Therefore, the energy used to degrade textile dye waste is energy in the system (Aziztyana et al., 2019).

3.5 Effect of Fe_3O_4 Concentration on Degradation of Batik Liquid Waste

The effect of Fe_3O_4 concentration in Fe_3O_4-SiO_2 and Fe_3O_4-SiO_2-Alginate was carried out by preparing 25 mL of textile dye waste in a beaker and then adding a photocatalyst containing Fe_3O_4-SiO_2 (powder) and Fe_3O_4-SiO_2-Alginate (granules) with varying concentrations of 5; 10; and 15% (w/w). The photocatalyst was then irradiated with visible light for 1 hour. Measurement of COD value was carried out on textile dye waste before and after degradation. The COD value of textile dye waste before degradation is 1160-1180 mg/L. Based on Figure 7 shows the effect of the concentration of Fe_3O_4 in Fe_3O_4-SiO_2 and Fe_3O_4-SiO_2-Alginate on the degradation of textile dye waste. The concentration of Fe_3O_4 can increase the degradation of textile dye waste. At a concentration of 15% Fe_3O_4 in the form of powder and granules, resulted in 84.48% and 79.66% degradation, respectively.

Figure 8 shows that variations in Fe_3O_4-SiO_2 concentration affect the percent decrease in COD value from textile dye waste. The results of this study indicate that the percent decrease in the COD value of textile dye waste increases with increasing Fe_3O_4 concentration. The higher the concentration, the higher the amount of •OH and the ability of the photocatalyst to degrade, and thus, the faster the process of breaking the bonds of the azo structure from the dye pollutant source and causing the COD value of textile dye waste to decrease and the color to be clearer (Aziztyana et al., 2019; Kabir et al., 2020).

© 2023 The Authors.

4. CONCLUSION

FTIR results showed that the Fe_3O_4-SiO_2-Alginate photocatalyst had absorption at wavelengths of 556.22 cm^{-1} and 3365.86 cm^{-1} which indicated the Fe-O-Si functional group and stretching vibration O-H. Analysis of the results of UV-Vis DRS, that the band gap energy for Fe_3O_4 was 2.20 eV and Fe_3O_4-SiO_2 was 1.77 eV. XRD results for Fe_3O_4 in the magnetite phase and the synthesized SiO_2 in the cristobalite phase with amorphous properties, and the photocatalyst with the highest degradation percentage of 84.48% is Fe_3O_4-SiO_2 15% with a long irradiation time of 60 minutes. The addition of alginate in the photocatalyst modification into granules did not affect the photocatalytic activity in the degradation of textile dye waste.

5. ACKNOWLEDGMENT

The author would like to thank the Chemistry Department, Brawijaya University, which has provided the willingness of the laboratory to carry out this project.

REFERENCES

Al-Anbari, R., A. H. Al Obaidy, and E. Abd (2016). Photocatalytic Activity of Fe3O4 Under Solar Radiation. *Mesopotamia Environmental Journal*, **2**(4); 41–53

Ardiyanti, H., D. Puspitarum, O. Maryana, and W. Pujakesuma (2019). Synthesis and Bonding Analysis of Magnetite (Fe3o4)/silica (Sio2) Composite Based on Sugarcane Bagasse. *Journal of Science and Applicative Technology*, **2**(1); 197–200

Asab, G., E. A. Zereffa, and T. Abdo Seghne (2020). Synthesis of Silica-coated Fe3O4 Nanoparticles by Microemulsion Method: Characterization and Evaluation of Antimicrobial Activity. *International Journal of Biomaterials*, **2020**(6); 1–11

Aziztyana, A. P., S. Wardhani, Y. P. Prananto, and D. Purwonugroho (2019). Optimisation of Methyl Orange Photodegradation Using TiO2-zeolite Photocatalyst and H2O2 in Acid Condition. *Materials Science and Engineering*, **546**(4); 042047

Bayat, M., V. Javanbakht, and J. Esmaili (2018). Synthesis of Zeolite/Nickel Ferrite/Sodium Alginate Bionanocomposite Via a co-precipitation Technique for Efficient Removal of Water-soluble Methylene Blue Dye. *International Journal of Biological Macromolecules*, **116**(7); 607–619

Benali, F., B. Boukoussa, I. Ismail, M. Hachemaoui, J. Iqbal, I. Taha, Z. Cherifi, and A. Mokhtar (2021). One Pot Preparation of CeO2@ Alginate Composite Beads for the Catalytic Reduction of MB Dye: Effect of Cerium Percentage. *Surfaces and Interfaces*, **26**(2); 101306

Chang, H., Q. Lin, M. Cheng, K. Zhang, B. Feng, J. Chai, Y. Lv, and Z. Men (2022). Effects of Potassium Loading Over Iron–Silica Interaction, Phase Evolution and Catalytic Behavior of Precipitated Iron-Based Catalysts for Fischer-Tropsch Synthesis. *Catalysts*, **12**(8); 916

Dhaneswara, D., J. F. Fatriansyah, F. W. Situmorang, and A. N. Haqoh (2020). Synthesis of Amorphous Silica from Rice Husk ash: Comparing HCI and CH3COOH Acidification Methods and Various Alkaline Concentrations. *Synthesis*, **11**(1); 200–208

Fatimah, I., F. U. Zaenuri, L. N. Doewandono, A. Yahya, P. W. Citradewi, S. Sagadevan, and W. C. Oh (2021). Biogenic Silica Extracted from Salacca Leaves Ash for the Adsorption of Salycilic Acid. *Science and Technology Indonesia*, **6**(4); 296–302

Gong, T. and Y. Tang (2020). Preparation of Multifunctional Nanocomposites $Fe_3O_4@SiO_2$–EDTA and its Adsorption of Heavy Metal Ions in Water Solution. *Water Science and Technology*, **81**(1); 170–177

Gunlazuardi, J., A. Fisli, R. Ridwan, Y. K. Krisnandi, and D. Robert (2021). Magnetically Separable Fe3O4/SiO2/TiO2 Photocatalyst Composites Prepared Through Hetero Agglomeration for the Photocatalytic Degradation of Paraquat. *Makara Journal of Science*, **25**(4); 6

Hedayati, K., M. Goodarzi, and D. Ghanbari (2017). Hydrothermal Synthesis of Fe3O4 Nanoparticles and Flame Resistance Magnetic Poly Styrene Nanocomposite. *Journal of Nanostructures*, **7**(1); 32–39

Kabir, R., M. A. K. Saifullah, A. Z. Ahmed, S. M. Masum, and M. A. I. Molla (2020). Synthesis of n-doped zno Nanocomposites for Sunlight Photocatalytic Degradation of Textile Dye Pollutants. *Journal of Composites Science*, **4**(2); 49

Kamari, S. and F. Ghorbani (2021). Extraction of Highly Pure Silica from Rice Husk as an Agricultural By-product and Its Application In the Production of Magnetic Mesoporous Silica MCM–41. *Biomass Conversion and Biorefinery*, **11**(6); 3001–3009

Keshavarz, M., M. Ottesen, S. Wiedmann, M. Wharmby, R. Küchler, H. Yuan, E. Debroye, J. A. Steele, J. Martens, and N. E. Hussey (2019). Tracking Structural Phase Transitions in Lead-Halide Perovskites by Means of Thermal Expansion. *Advanced Materials*, **31**(24); 1900521

Kouotou, P. M., A. El Kasmi, L. N. Wu, M. Waqas, and Z. Y. Tian (2018). Particle Size Band Gap Energy Catalytic Properties Relationship of PSE CVD Derived Fe3O4 Thin Films. *Journal of the Taiwan Institute of Chemical Engineers*, **93**(3); 427–435

Luthfiah, A., Y. Deawati, M. L. Firdaus, I. Rahayu, and D. R. Eddy (2021). Silica from Natural Sources: a Review on the Extraction and Potential Application as a Supporting Photocatalytic Material for Antibacterial Activity. *Science and Technology Indonesia*, **6**(3); 144–155

Madima, N., K. K. Kefeni, S. B. Mishra, A. K. Mishra, and A. T. Kuvarega (2022). Fabrication of Magnetic Recoverable Fe_3O_4/TiO_2 Heterostructure for Photocatalytic Degradation of Rhodamine B dye. *Inorganic Chemistry Communications*, **145**; 109966

Mohammadi, R. and N. Sabourmoghaddam (2019). Adsorption of Azo Dye Methyl Orange from Aqueous Solutions Using TiO2-SiO2/Alginate Nanocomposite. *Asian Journal*

© 2023 The Authors.

of Green Chemistry, **4**(1); 107–120

Nikmah, A., A. Taufiq, and A. Hidayat (2019). Synthesis and Characterization of Fe3O4/SiO2 Nanocomposites. *Earth and Environmental Science*, **276**(1); 012046

Nisaa, A. K., S. Wardhani, and D. Purwonugroho (2018). Tempe Waste Water Degradation Using TiO2-N/Bentonite alginate Granule Photocatalyst with Ultraviolet Light Irradiation. *Materials Science and Engineering*, **299**(1); 012030

Sapei, L., K. S. Padmawijaya, A. Sutejo, and L. Theresia (2015). Karakterisasi Silika Sekam Padi dengan Variasi Temperatur Leaching Menggunakan Asam Asetat. *Jurnal Teknik Kimia*, **9**(2); 38–43 (In Indonesia)

Saragi, T., B. Permana, M. Saputri, L. Safriani, and R. Iman Rahayu (2018). Karakteristik Optik dan Kristal Nanopartikel Magnetit. *JIIF (Jurnal Ilmu dan Inovasi Fisika)*, **2**(1); 53–56 (In Indonesia)

Song, N. N., H. T. Yang, H. L. Liu, X. Ren, H. F. Ding, X. Q. Zhang, and Z. H. Cheng (2013). Exceeding Natural Resonance Frequency Limit of Monodisperse Fe3O4 Nanoparticles Via Superparamagnetic Relaxation. *Scientific Reports*, **3**(1); 1–5

Ta, T. K. H., M. T. Trinh, N. V. Long, T. T. M. Nguyen, T. L. T. Nguyen, T. L. Thuoc, B. T. Phan, D. Mott, S. Maenosono, and H. Tran Van (2016). Synthesis and Surface Functionalization of Fe3O4-SiO2 Core Shell Nanoparticles with 3-glycidoxypropyltrimethoxysilane and 1, 1-carbonyldiimidazole for Bio-applications. *Colloids and Surfaces A: Physicochemical and Engineering Aspects*, **504**(8); 376–383

Tak, B. y., B. s. Tak, Y. j. Kim, Y. J. Park, Y. h. Yoon, and G. h. Min (2015). Optimization of Color and COD Removal from Livestock Wastewater by Electrocoagulation Process: Application of Box–Behnken Design (BBD). *Journal of Industrial and Engineering Chemistry*, **28**(4); 307–315

Thiyagarajan, R., X. Yan, V. Pazhanivelu, A. P. B. Selvadurai, R. Murugaraj, and W. Yang (2018). Doping Effect of Alkali Metal Elements on the Structural Stability and Transport Properties of ZnO at High Pressures. *Journal of Alloys and Compounds*, **751**(5); 266–274

Villegas, V. A. R., J. I. D. L. Ramírez, E. H. Guevara, S. P. Sicairos, L. A. H. Ayala, and B. L. Sanchez (2020). Synthesis and Characterization of Magnetite Nanoparticles for Photocatalysis of Nitrobenzene. *Journal of Saudi Chemical Society*, **24**(2); 223–235

Yuliasari, N., R. M. Amri, and A. L. Elfita (2021). Improvement of Congo Red Photodegradation Performance Through Zn/Al-TiO2 and Zn/Al-ZnO Preparation. *Science and Technology Indonesia*, **7**(4); 449–454

© 2023 The Authors.